MOLECULAR AND CELLULAR BIOLOGY, Dec. 2003, p. 8505–8518 Vol. 23, No. 23
0270-7306/03/$08.00+0 DOI: 10.1128/MCB.23.23.8505–8518.2003

Nonhomologous-End-Joining Factors Regulate DNA Repair Fidelity during *Sleeping Beauty* Element Transposition in Mammalian Cells

Stephen R. Yant and Mark A. Kay*

Departments of Pediatrics and Genetics, Stanford University School of Medicine, Stanford, California

Received 8 May 2003/Returned for modification 15 July 2003/Accepted 14 August 2003

Herein, we report that the DNA-dependent protein kinase (DNA-PK) regulates the DNA damage introduced during *Sleeping Beauty* (*SB*) element excision and reinsertion in mammalian cells. Using both plasmid- and chromosome-based mobility assays, we analyzed the repair of transposase-induced double-stranded DNA breaks in cells deficient in either the DNA-binding subunit of DNA-PK (Ku) or its catalytic subunit (DNA-PK_{cs}). We found that the free 3′ overhangs left after *SB* element excision were efficiently and accurately processed by the major Ku-dependent nonhomologous-end-joining pathway. Rejoining of broken DNA molecules in the absence of Ku resulted in extensive end degradation at the donor site and greatly increased the frequency of recombination with ectopic templates. Therefore, the major DNA-PK-dependent DNA damage response predominates over more-error-prone repair pathways and thereby facilitates high-fidelity DNA repair during transposon mobilization in mammalian cells. Although transposable elements were not found to be efficiently circularized after transposase-mediated excision, DNA-PK deficiency supported more-frequent transposase-mediated element insertion than was found in wild-type controls. We conclude that, based on its ability to regulate excision site junctional diversity and transposon insertion frequency, DNA-PK serves an important protective role during transpositional recombination in mammals.

The use of transposable elements as genetic tools has contributed significantly to our understanding of biological systems. The Tc1/*mariner* elements are likely the most widespread transposons in nature and can transpose in species other than their hosts, making them potential tools for functional genomics in diverse organisms, including vertebrates (48). However, most naturally occurring Tc1/*mariner*-like transposons are nonfunctional due to the accumulation of inactivating mutations (36). Although no single active element has ever been identified in vertebrates, an active Tc1-like transposon called *Sleeping Beauty* (*SB*) was recently reconstructed from pieces of defective fish elements (23). *SB* functions in a variety of vertebrate species, including human and mouse cells (24), and is the most active member of the Tc1/*mariner* family (16). Moreover, this element has been applied recently to gene discovery in the mouse germ line (13, 14, 16, 21) and has been shown to promote stable in vivo delivery of therapeutic genes in somatic tissues of adult mice (41, 65, 66). Based on emerging interest in further developing such tools for basic research and therapeutic applications, studies which elucidate the molecular mechanisms involved in transposition and its regulation in mammals remain of significant importance.

Each end of *SB* contains an inverted repeat (IR)-direct repeat (DR) structure consisting of two short DRs within an ~230-bp imperfect terminal IR. These DRs (~30 bp) serve as core binding sites for the element-encoded transposase (23), and the presence of both sites within an individual IR is required for efficient transposition (24). In addition to the DRs, the left IR of *SB* contains a half binding site, termed HDR, which acts as a transpositional enhancer-like sequence (25). Specific binding to the DRs is mediated by an N-terminal, paired-domain-like DNA-binding domain of the transposase (23, 25). The C-terminal, catalytic domain of the transposase is responsible for all DNA cleavage and strand transfer reactions and is characterized by the presence of a conserved amino acid triad, the DDE motif. This catalytic triad is found in a large group of recombinases, including many eukaryotic and bacterial transposases, retroviral integrases, and the RAG1 V(D)J recombinase, involved in immunoglobulin gene rearrangements (50).

Like V(D)J recombination, the mobilization of *SB* elements is a specialized form of DNA recombination and occurs by a cut-and-paste pathway involving a DNA intermediate. This transposition process involves five distinct stages, the first four of which include (i) association of the transposase with its binding sites within the transposon IRs, (ii) assembly of an active synaptic complex in which the two ends of the element are paired and held together by bound transposase subunits, (iii) transposase-mediated excision of the element from its original donor site, and (iv) reinsertion of the excised element into a new target site (TA dinucleotide). This joining step occurs when the 3′ hydroxyl (3′ OH) at each end of the excised element performs a nucleophilic attack on the host DNA, producing an integration intermediate that contains single-strand gaps in the flanking host DNA sequence. In the final stage of the transposition process, the noncomplementary ends of the broken donor DNA molecule are processed and rejoined and the gaps are filled at the insertion site. These repair processes generate a small excision site footprint, consisting of a few base pairs of transposon end sequence, as well as a characteristic duplication of the target TA dinucleotide at the insertion site (Fig. 1). Although it is generally assumed that host repair enzymes remove the DNA damage produced dur-

* Corresponding author. Mailing address: Stanford University School of Medicine, Department of Pediatrics, 300 Pasteur Dr., Room G-305, Stanford, CA 94305-5208. Phone: (650) 498-6531. Fax: (650) 498-6540. E-mail: markay@stanford.edu.

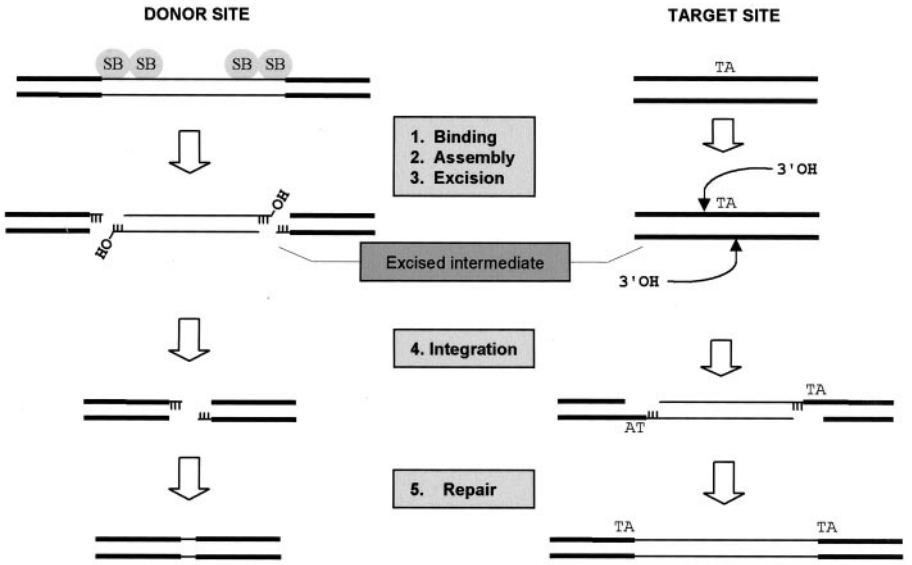

FIG. 1. Requirement for DNA repair during transposition of *SB* elements. An *SB* element is excised by transposase via sequential 3-bp staggered cuts at the ends of the inverted terminal repeats, completely releasing it from its original donor site. This newly excised element then integrates into a TA target site via a series of transesterification reactions such that the TA is duplicated at the ends of the element following repair of the single-stranded DNA gaps. Depending on how the DSB at the site of excision is repaired, a small transposon footprint will sometimes be left behind.

ing *SB* element transposition in mammalian cells, the identity of the specific host factor(s) involved in these important processes has not been clearly defined.

The repair of DNA damage, especially double-stranded DNA breaks (DSBs), is critical for the maintenance of genomic stability. If DNA DSBs are left unrepaired or are repaired inaccurately, mutations and/or chromosomal aberrations are induced, which in turn may lead to cell death or, in extreme cases, cancer. Eukaryotic cells have evolved two major mechanisms to contend with these DSBs. In homologous recombination, repair of a broken DNA molecule is directed by an intact homologous duplex. Alternatively, the ends of broken DNA molecules are rejoined without the need for substantial DNA sequence homology by a process known as nonhomologous DNA end joining (NHEJ). The latter pathway appears to be the prevailing mechanism for DSB repair in mammalian cells (30) and has been shown to be involved in both V(D)J recombination (57) and retrovirus DNA integration (10, 11, 33).

Genetic and biochemical studies of mammalian cells have identified several factors involved in the NHEJ pathway. These include the DNA-dependent protein kinase catalytic subunit (DNA-PK_{cs}), the Ku70/Ku80 heterodimer, Artemis, and the DNA ligase IV/XRCC4 complex (28). In response to a DSB, Ku heterodimers bind to and facilitate the initial alignment of the two DNA termini and then stimulate the recruitment of DNA-PK_{cs}, thus forming an active DNA-PK complex (20). DNA-PK_{cs} also forms a physical complex with Artemis, which alone possesses 5′-to-3′ exonuclease activity (39). Upon complex formation, DNA-PK_{cs} phosphorylates Artemis, which consequently acquires endonucleolytic activity on 5′ and 3′ overhangs, as well as hairpins, including those generated by the RAG complex during V(D)J recombination (39). Finally, biochemical fractionation studies suggest that the Mre11/Rad50/NBS1 (MRN) complex, which exhibits both nuclease and DNA end-bridging activity in vitro, may play a key role in aligning DNA ends in a synaptic complex immediately prior to ligation by the DNA ligase IV/XRCC4 complex (8, 22).

In this report, we investigated what role, if any, NHEJ plays in the response to DNA transposition in mammalian cells. We triggered *SB* element mobilization from extrachromosomal plasmids in Ku- or DNA-PK_{cs}-deficient and wild-type control cells by expressing the *SB* transposase in *trans* from a transfected plasmid. We then studied the requirement for DNA-PK in gap repair during transposon integration and in the rejoining of DSBs produced at excision sites. Herein we show efficient transposon integration in the soma of DNA-PK-deficient *scid* mice and in rodent cells lacking either Ku or DNA-PK_{cs}, suggesting that DNA-PK activity is not essential for proper DNA repair after transposon insertion. We report that, instead, DNA-PK activity, especially its regulatory component (Ku), is necessary for proper rejoining of the double-stranded DNA gaps left after *SB* element excision in mammals. DNA transposition in the absence of Ku was highly error prone, resulting in significant degradative loss of the individual DNA termini and frequent recombination with ectopic templates. Interestingly, similar types of misrepair events were also observed after inducing chromosomal transposition in a wild-type human cell line, suggesting that transposase activity might facilitate recombination activity in vertebrates. These studies reveal additional parallels between *SB* element excision and V(D)J recombination and suggest a potential role for transposition-induced recombination in the evolution of vertebrate genomes.

MATERIALS AND METHODS

Animals studies. We obtained 6- to 8-week-old C57BL/6 and DNA-PK(−) C57BL/6-*scid* mice from Jackson Laboratory. Animals were treated according to

the National Institutes of Health guidelines for animal care and the guidelines of Stanford University. Mice were anesthetized with isoflurane (Abbott Laboratories) for surgical partial hepatectomy, which uniformly induces one or two rounds of hepatic cell division throughout the liver over a period of 3 weeks. Plasmid DNAs were delivered to mice by hydrodynamics-based transfection as previously described (35, 69). We collected mouse serum from the retro-orbital plexus and analyzed it by an enzyme-linked immunosorbent assay (ELISA) for total hAAT antigen as previously described (26).

Plasmid construction. Plasmids pCMV-SB, pCMV-mSB, pCMV-GFP, pTnori, phAAT, and pThAAT have all been previously described (66). For the purposes of our methylation-sensitive Southern blot analyses, we isolated pThAAT from both DH10B (*dam*-positive) and GM48 (*dam*-negative) bacterial host strains. The plasmid pTpuro containing a PGK-driven puromycin-marked transposon was made by inserting a 1.7-kb *Sal*I fragment from pPGK-Puro (kindly provided by P. Laird, Whitehead Institute) into *Xho*I-treated pT-MCS (66). To produce the lentivirus-based reporter construct pLNTH-15, we first produced an *SB* transposon containing a hygromycin expression cassette by inserting a 2-kb *Bsm*I fragment from pTK-Hyg (Clontech) into *Xho*I/*Bsm*I-treated pT-MCS by blunt end ligation.

Southern blot analysis of transposon integration in mouse liver. We purified the pThAAT vector from *dam*-positive bacteria and injected it (25 μg) into both C57BL/6 and C57BL/6-*scid* mice together with 1 μg of either pCMV-SB ($n = 6$ mice) or pCMV-mSB ($n = 3$ mice). Ten months after vector administration, we performed a surgical partial (two-thirds) hepatectomy in order to facilitate demethylation of *Dpn*I recognition sites within integrated copies of the transposon. Forty-five days later, mice were sacrificed and liver DNA was prepared by a salting out method. For Southern blot analyses, we digested 10 μg of mouse liver DNA with *Dpn*I, *Hin*dIII (cuts twice within the transposon), or *Dpn*I and *Hin*dIII together and then separated it by ethidium bromide agarose gel electrophoresis and transferred it to nitrocellulose. Membranes were hybridized to a radiolabeled 1.7-kb hAAT fragment and subjected to autoradiography.

Cells and cell culture. HeLa, 293-T, V79-4 (hamster lung), Ku86-deficient CHO-K1-derived (*xrs-5*), and V79-4-derived (XR-V15B) cell lines were all obtained from the American Type Culture Collection and were cultured in Dulbecco's modified Eagle's medium (DMEM) containing high glucose, 10% fetal bovine serum (FBS), 1× penicillin-streptomycin, and 4 mM L-glutamine. S-MHB-2 and C-MHB-2 cells were kindly provided by C. Kirchgessner (Stanford University) and are derived from transformed fibroblasts from ST.SCID mice and congenic C.B-17 parent mice, respectively (51). These cells were grown in the same medium supplemented with 500 μg of Geneticin (Gibco, BRL)/ml. CHO-K1 (hamster ovary) cells were grown in Kaighn's modification of Ham's F-12 medium with 10% FBS. All cell lines were maintained at 37°C in a humidified atmosphere of 5% CO_2.

Assay for transposition in mammalian cells. We used a genetic assay to study transposition in the presence and absence of known cellular DNA repair factors. HeLa, CHO-K1, *xrs-5*, V79-4, and XR-V15B cells were all plated on six-well dishes the day before cotransfection with a plasmid containing a neomycin gene-marked transposon (pTnori) together with either pCMV-SB or pCMV-mSB as a control using Superfect (Qiagen). Transfected cells were trypsinized 2 days later, diluted into DMEM containing 600 μg of G418/ml, and growth selected for a period of 2 weeks. At this time, G418-resistant ($G418^R$) colonies were fixed, stained, and counted to determine the relative amount of transposase-mediated integration in each cell line. To study transposition in S-MHB-2 and C-MHB-2 cells, which already contain a *neo* cassette from previous studies (51), we substituted a plasmid containing a puromycin gene-marked transposon (pTpuro) for pTnori and performed growth selection in DMEM containing 5 μg of puromycin/ml. In every case, transfections were done in triplicate and produced similar results.

Establishment of chromosomal transposition reporter cell lines. We studied the repair of transposase-induced DSB in host cell chromosomes using a lentivirus-based reporter system to detect rare excisions from various chromosomal loci. To do this, we first produced a replication-defective human immunodeficiency virus type 1 (HIV-1)-based vector (LNTH) containing a transposition-dependent reporter construct by a triple-transfection procedure (44). Briefly, we transfected a 10-cm-diameter dish of 293-T cells by the calcium phosphate method with 3.5 μg of pMD.G, 6.5 μg of pCMVΔ8.74, and 10 μg of pLNTH-15 in the presence of 27.5 μM chloroquine. The medium was changed 8 h later, and virus-containing medium was harvested 40 h posttransfection. Virus was titered by an ELISA method (Alliance; Dupont-NEN) that determines the HIV p24 Gag antigen concentration.

We infected HeLa and Ku86-deficient XR-V15B cells with the LNTH reporter virus at a low multiplicity of infection (0.1). Two days later, we trypsinized these cells and diluted them into DMEM containing 300 μg of hygromycin B (Gibco, BRL)/ml for growth selection for at least 2 weeks. Individual hygromycin-resistant (Hyg^R) colonies were picked, amplified, and screened for complete sensitivity to G418 drug selection in the absence of transposase expression. Genomic DNA was prepared from each Hyg^R $G418^S$ clone by a salting out procedure and subjected to Southern blot analyses following treatment with either *Bgl*I (cuts once) or *Ava*I (cuts twice) to identify clones containing a single full-length copy of the testing construct at different chromosomal loci. Four HeLa-derived and eight XR-V15B-derived clones were expanded for further analysis.

To trigger excision of the *SB* element from these chromosomal sites, we transfected ~10^7 cells from each reporter line with 20 μg of pCMV-SB or pCMV-GFP as a control using Superfect (Qiagen). Transfection efficiencies for both cell types were analyzed the next day by fluorescence microscopy and found to be ~15%. Three days after transfection, transposase- and green fluorescent protein (GFP)-expressing cells were growth selected for 3 weeks in DMEM containing 600 μg of G418/ml. Each G418-resistant colony (produced only from HeLa-derived pCMV-SB-transfected cultures) was picked and expanded for further analysis.

PCR, Southern blotting, and expression-based analyses of transposon reinsertion. To characterize the frequency of transposon reinsertion following *SB*-mediated transposon excision, we analyzed the genome of each $G418^R$ clone by PCR for the presence of the transposon using oligonucleotide primers Hyg-1A (5′-GAGGCCATGGATGCGATCGCTGCG) and Hyg-1B (5′-ATTGCGTCG CATCGACCCTGCGCC). The proportion of $G418^R$ clones that supported growth in DMEM containing 300 μg of hygromycin/ml was determined to estimate the frequency of transposon silencing following transposon reinsertion into random chromosomal sites. The diversity of reinsertion sites was analyzed by genomic Southern blot analysis of $G418^R$ clones using *Spe*I (cuts once) and a radiolabeled probe specific for the transposon.

PCR and sequence analysis of DSB repair products following SB element excision. We studied the repair of DNA DSBs following transposon excision from extrachromosomal plasmid DNA in both cultured mammalian cells and in the somatic tissue of adult mice. To do this, we cotransfected Ku86-expressing (V79-4 and CHO-K1) and Ku86-deficient (XR-V15B and *xrs-5*) cell lines with pTnori and either pCMV-SB or pCMV-mSB as a control and then performed a standard Hirt DNA extraction 30 h later. To study in vivo DSB repair in the presence and absence of DNA-PK activity, we also injected C57BL/6 and C57BL/6-*scid* mice via the tail vein with 25 μg of pThAAT or a control vector (phAAT) together with 1 μg of either pCMV-SB or pCMV-mSB and then isolated total liver DNA either 2 days or 30 days later by salting out. In each of these studies, we used 500 ng of DNA together with oligonucleotide primers puc1 (5′-TACG CCAGCTGGCGAAAG) and puc2 (5′-AGCTCACTCATTAGGCAC) to amplify excision repair products. PCR products were analyzed by ethidium bromide gel electrophoresis, excised, and cloned into the pCR4-TOPO vector (Invitrogen) for DNA sequence analysis. To characterize the repair pathways involved in rejoining transposase-induced DSBs in host cell chromosomes, we amplified a DNA segment encompassing the transposon donor site from the genome of HeLa-derived G418-resistant LNTH clones using oligonucleotide primers HIV-1A (5′-CAGCTCCAGGCAAGAATCCTG) and NEO-1 (5′-GCCCAGTC AAGCCGAATAGCC). Each PCR product was analyzed by ethidium bromide gel electrophoresis, gel purified, and subjected to direct DNA sequencing.

RESULTS

Efficient integration of *SB* elements in the liver of DNA-PKcs-deficient *scid* mice. We studied what role, if any, DNA-PK plays in *SB* element transposition in vivo by analyzing transposon excision and chromosomal reinsertion in normal and DNA-PK-deficient mice. To do this, we injected C57BL/6 mice and genetically matched *scid* mice (containing a DNA-PKcs truncation mutation in both alleles) via the tail vein with an *SB* transposon plasmid containing a human α_1-antitrypsin expression cassette (pThAAT) flanked by the IR-DR structure (Fig. 2A) together with a transposase plasmid encoding either the wild-type *SB* transposase (pCMV-SB) or a catalytically inactive mutant transposase (pCMV-mSB) as a control. Compared with pCMV-mSB-injected control mice, both normal (data not shown) and DNA-PK-deficient *scid* mice (Fig. 2B) expressed ~65-fold more serum hAAT for a period of 10 months. Importantly, expression in *scid* mice

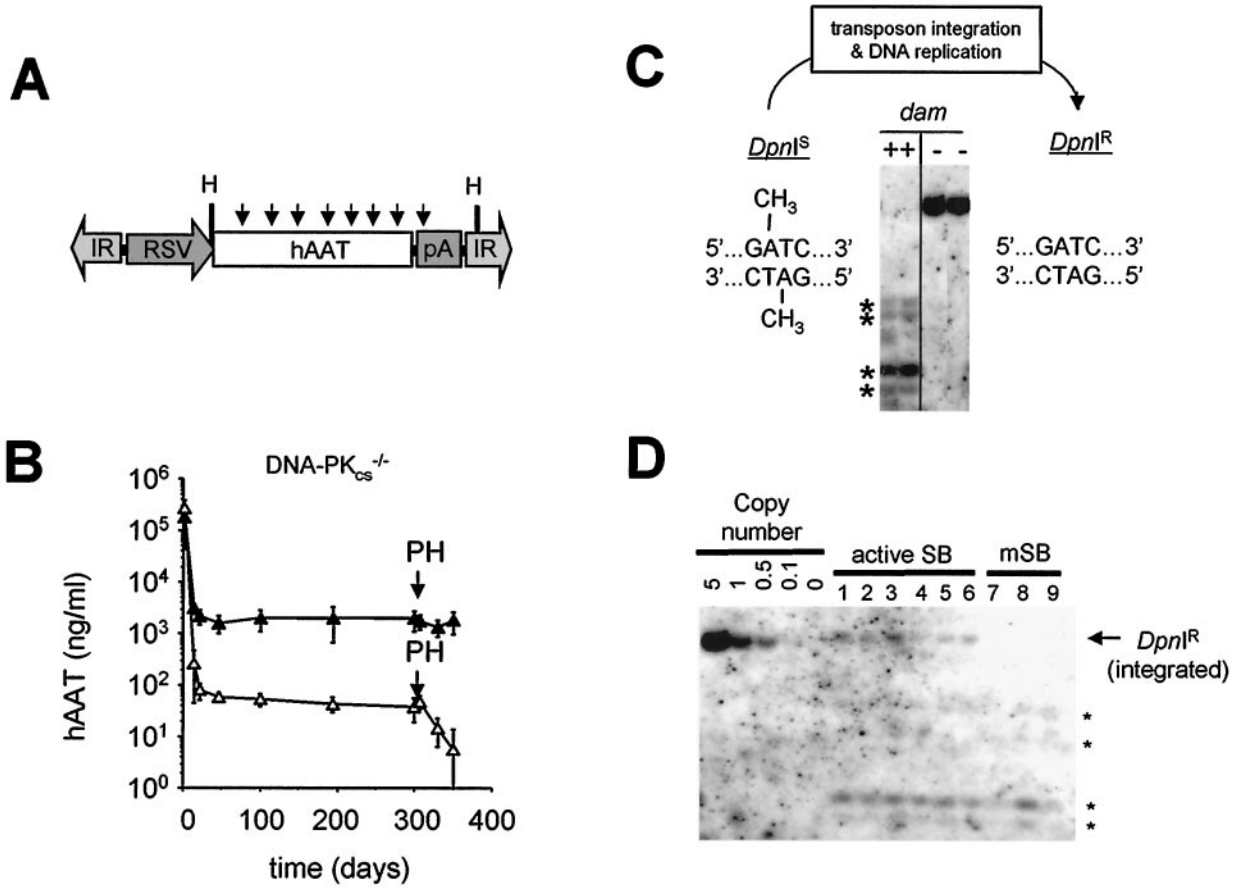

FIG. 2. Stable integration and expression of *SB* elements in mice in the absence of DNA-PK activity. (A) Schematic of the *Dpn*I-sensitive hAAT transposon injected into mice. The vector pThAAT was purified from bacteria expressing the *dam*-encoded methylase, making it susceptible to digestion with the restriction endonuclease *Dpn*I. Arrows, locations of *Dpn*I recognition sites, which are substrates for *Dpn*I only when the internal adenine residue is methylated. RSV, Rous sarcoma virus long terminal repeat promoter; hAAT, human α_1-antitrypsin cDNA; IR, *SB* element IR sequence; H, *Hin*dIII. (B) Transposon-based human α_1-antitrypsin expression in DNA-PK_{cs}-deficient *scid* mice before and after a surgical partial hepatectomy (PH). Immune-deficient C57BL/6-*scid* mice were injected with 25 μg of pThAAT together with 1 μg of either pCMV-SB (▲) (contains wild-type *SB*; $n = 6$ mice) or pCMV-mSB (△) (contains inactive *SB*; $n = 3$ mice) as a control, and their serum hAAT levels were monitored over time by ELISA. Liver regeneration was induced 10 months after vector administration by surgically removing two-thirds of the mouse liver under anesthesia. (C) Southern blot analysis of *Dpn*I-treated control DNA purified from *dam*-positive and *dam*-negative bacteria. We used mouse liver DNA (10 μg) spiked with 0.1 ng of methylated (*dam*-positive) or unmethylated (*dam*-negative) vector DNA for Southern blot analysis. Membranes were probed with a radiolabeled hAAT fragment. Asterisks, cleavage fragments derived from *Dpn*I-treated input vector. (D) Methylation-sensitive Southern blot analysis of mouse liver DNA obtained 11.5 months after vector administration. We used 10 μg of total liver DNA digested with *Dpn*I and *Hin*dIII for Southern blot analysis and hybridized membranes to a radiolabeled hAAT probe. The left five lanes (5.0 to 0.1 copies/cell) were derived from adding a *dam*-negative (*Dpn*I-resistant) pThAAT plasmid to mouse liver DNA. Arrow, integrated, *Dpn*I-resistant copies of the transposon in pCMV-SB-treated animals; asterisks, presence of *Dpn*I-sensitive transposon episomes in all samples.

treated with active transposase remained essentially unchanged during a 4-week time period following a partial (two-thirds) surgical hepatectomy, which is consistent with stable chromosomal integration irrespective of DNA-PK activity. To confirm these findings at the molecular level, we performed Southern blot analyses using the restriction endonuclease *Dpn*I to differentiate between episomal and integrated forms of transposon DNA in these mice. Since this enzyme recognizes the methylated sequence GmATC, which is present eight times within the transposon portion of the pThAAT vector (Fig. 2A), extrachromosomal forms of the vector are completely digested, whereas integrated transposon copies that have undergone sufficient replication to completely demethylate these *Dpn*I sites remain resistant to *Dpn*I cleavage (Fig. 2C). Using this approach, we analyzed DNA from the livers of both normal ($n = 9$) and DNA-PK-deficient ($n = 9$) *scid* mice. Irrespective of the presence or absence of DNA-PK activity, mice which received active transposase contained an average of 0.25 copies of *Dpn*I-resistant transposon DNA per diploid liver genome (Fig. 2D and data not shown). These data suggest that DNA-PK activity is not required in vivo for stable transposase-mediated insertion into host cell chromosomes.

Efficient, low-fidelity DSB repair in vivo in the absence of DNA-PK activity. We monitored *SB* element excision and DSB repair in the livers of normal and DNA-PK-deficient *scid* mice using a PCR approach. This assay utilizes primers located outside of the transposon such that excision of the transposon brings the two primers close enough together for PCR ampli-

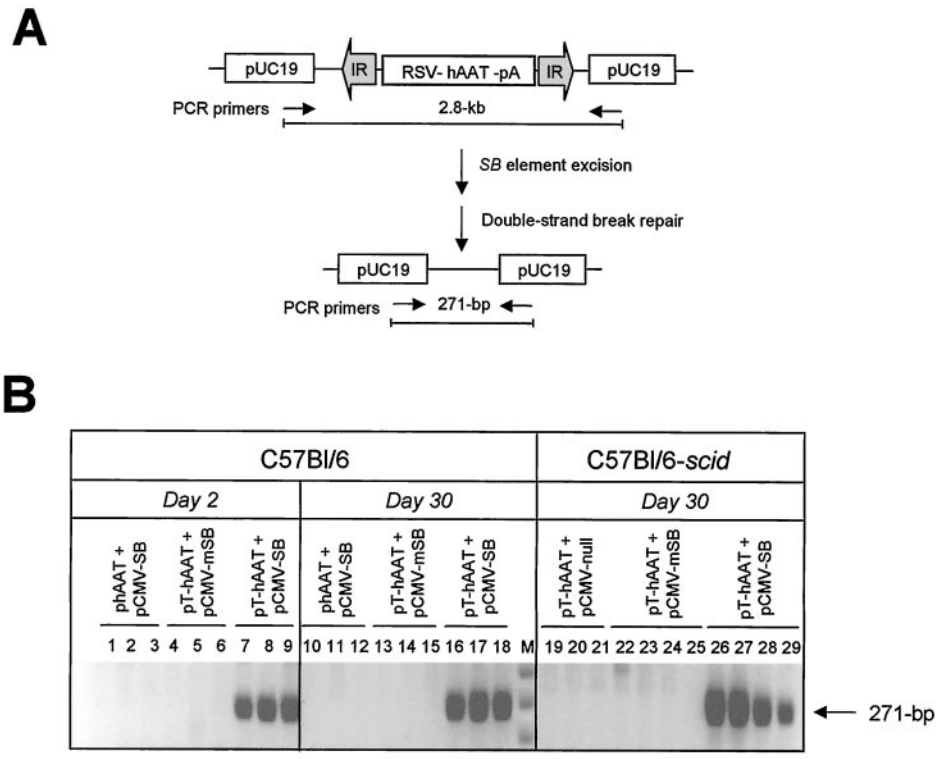

C

	C57Bl/6	NO:	Ftpnt(bp):	Del(bp):
DNA-PK(+) (n=23)	TGAATTCGAG CTCGGTACCC TA ctgTA GGGGATCCTC TAGAGTCGAC	9	3	0
	TGAATTCGAG CTCGGTACCC TAcag TA GGGGATCCTC TAGAGTCGAC	7	3	0
	TGAATTCGAG CTCGGTACCC TAtgt TA GGGGATCCTC TAGAGTCGAC	1	3	0
	TGAATTCGAG CTCGGTACCC TA ttgTA GGGGATCCTC TAGAGTCGAC	1	3	0
	TGAATTCGAG CTCGGTACCC TAcgt TA GGGGATCCTC TAGAGTCGAC	1	3	0
	TGAATTCGAG CTCGGTACCC TAca TA GGGGATCCTC TAGAGTCGAC	1	2	0
	TGAATTCGAG CTCGGTACCC TAccg TA GGGGATCCTC TAGAGTCGAC	1	3	0
	TGAATTCGAG CTCGGTA--- -- -- GGGGATCCTC TAGAGTCGAC	1	NA	7
	TGAAT----- ---------- -- -- ----ATCCTC TAGAGTCGAC	1	NA	23

	C57Bl/6-*scid*	NO:	Ftpnt(bp):	Del(bp):
DNA-PK(-) (n=23)	TGAATTCGAG CTCGGTACCC TA ttgTA GGGGATCCTCTAGAGTCGAC	1	3	0
	TGAATTCGAG CTCGGTACCC TA tgTA GGGGATCCTCTAGAGTCGAC	1	2	0
	TGAATTCGAG CTCGGTACCC TA agTA GGGGATCCTCTAGAGTCGAC	1	2	0
	TGAATTCGAG CTCGGTACCC TAca TA GGGGATCCTCTAGAGTCGAC	1	2	2
	TGAATTCGAG CTCGGTACCC TAca GGGGATCCTCTAGAGTCGAC	1	2	3
	TGAATTCGAG CTCGGTACCC -- gTA GGGGATCCTCTAGAGTCGAC	1	1	2
	TGAATTCGAG CTCGGTACCC -- TA GGGGATCCTCTAGAGTCGAC	1	NA	2
	TGAATTCGAG CTCGGTACCC -- -- GGGGATCCTCTAGAGTCGAC	2	NA	4
	TGAATTCGAG CTCGGTA--- -- TA GGGGATCCTCTAGAGTCGAC	1	NA	5
	TGAATTCGAG CTCGGTACCC T- TA GGGGATCCTCTAGAGTCGAC	2	NA	1
	TGAATTCGAG CTCGGTACCC TA TA GGGGATCCTCTAGAGTCGAC	5	NA	0
	TGAATTCGAG CTCGGTACCC TA -A GGGGATCCTCTAGAGTCGAC	1	NA	1
	TGAATTCGAG CTCGGTACC- -- -- ---GATCCTCTAGAGTCGAC	1	NA	8
	---------- ---------- -- -A GGGGATCCTCTAGAGTCGAC	1	NA	29
	---------- ---------- -- -- -GGGATCCTCTAGAGTCGAC	1	NA	73
	---------- ---------- -- -- GGGGATCCTCTAGAGTCGAC	1	NA	74
	---------- ---------- -- -- ----------	1	NA	96

FIG. 3. DNA-PK-independent repair of transposase-induced DSBs in vivo in mouse liver. (A) PCR-based strategy to detect repair of transposase-induced DSBs following transposon excision from donor plasmid constructs. The structure of the pThAAT vector DNA is shown in linear format for simplicity but was delivered to mice as a supercoiled plasmid. Prior to DNA transposition, PCR primers (arrows) are located 2.8 kb apart, which is beyond the PCR capacity. Following *SB*-mediated transposon excision and DSB repair, the primers are brought close enough together to allow PCR amplification. (B) Transposon excision and DSB repair in mouse liver. Normal C57BL/6 and DNA-PK_{cs}-deficient C57BL/6-*scid* mice received a donor hAAT vector with (pThAAT) or without (phAAT) transposase binding sites, together with either pCMV-SB or pCMV-mSB as a control. Total liver DNA was isolated at either day 2 or day 30 postinjection and analyzed by PCR for the presence of a 271-bp product of excision and repair. (C) Variety of DSB repair products produced in vivo in the presence (C57BL/6) and absence (C57BL/6-*scid*) of DNA-PK activity. The total numbers of clones with identical characteristics are shown, as well as the sizes in base pairs of both the resulting footprint and deleted region. Footprints are in lowercase. Dashes, deleted nucleotides; NA, not applicable.

fication (Fig. 3A). Transposase-specific repair products were detected in liver samples from normal C57BL/6 mice ($n = 3$) 2 days after coadministration of transposon-containing and transposase-encoding plasmids (Fig. 3B, lanes 7 to 9) and remained equally detectable after a period of 1 month (Fig. 3B, lanes 16 to 18). PCR amplification of DSB repair products from the livers of four DNA-PK-deficient *scid* mice produced equally strong bands, although they appeared slightly more diffuse than products generated from normal mice (Fig. 3B, lanes 26 to 29). These data suggest that repair of transposase-induced DSBs in mouse liver is rapid and efficient and does not require the activity of the DNA-PK complex.

We cloned and sequenced the region surrounding the excision site in order to characterize donor site end joining in the presence and absence of DNA-PK. The vast majority of repair products (20 of 23) isolated from normal mice showed no loss of neighboring sequences and contained a TA-flanked 3-bp footprint (Fig. 3C, top). These results are consistent with a 3-bp staggered cut-and-paste model for *SB*-mediated transposon excision previously reported (38). Of the remaining three clones, one contained a 2-bp footprint, while the other two contained short deletions of flanking DNA. In contrast, all 23 repair products isolated from DNA-PK-deficient mice showed tremendous diversity in the type of footprint left behind after transposon excision, as well as the frequency and length of DNA lost in the regions surrounding the transposase-induced DSB (Fig. 3C, bottom). Collectively, these results demonstrate that DNA-PK-dependent NHEJ is required for accurate processing of DSB produced in vivo during *SB* element transposition.

Deficiency of DNA-PK activity facilitates transposon integration in cultured mammalian cells. We used a genetic approach to investigate the requirement for DNA-PK activity in *SB* element transposition in cultured mammalian cells. To do this, we cotransfected normal and DNA repair-deficient mammalian cell lines with a plasmid containing a neomycin gene-marked transposon (pTnori) together with a helper plasmid encoding either active transposase (pCMV-SB) or catalytically inactive transposase (pCMV-mSB) as a control. We then quantified the number of stable integration events in each cell line following a 2-week growth selection in the antibiotic G418. Although cells deficient in either DNA-PK$_{cs}$ or Ku86 produced approximately 25% less total G418-resistant colonies than their normal parental controls, the ratio of transposase-mediated integration events to illegitimate recombination events was found to be ~1.6-fold higher in all DNA-PK-deficient cells than in their respective wild-type controls (Table 1). These results further demonstrate that DNA-PK-dependent NHEJ activity is not essential for stable transposition into mammalian cell chromosomes.

The presence of extrachromosomal transposon circles has been shown for other eukaryotic DNA elements (18, 59), including members of the Tc1/*mariner* family (3, 54, 55). Moreover, a recent report by Li et al. (33) showed that a subset of retroviral preintegration complexes are circularized in mammalian cells by DNA-PK-dependent NHEJ (33). We therefore tested whether DNA-PK limits the frequency of productive *SB* transposition in normal cells by converting a proportion of linear excised *SB* elements into circles via end-to-end joining. To do this, we isolated Hirt DNA from HeLa cells cotransfected with plasmids containing a transposon (pTnori) and either active or inactive transposase as a control. We then assayed for the presence of closed-circle transposon forms using two-step PCR together with nested primer pairs. Whereas molecules containing adjacent or nearby *SB* ends could be readily detected in a transposase-dependent manner, significantly more product was recovered from Ku-deficient cells than from normal cells, which is not consistent with reduced end joining of excised *SB* elements in the absence of DNA-PK. Indeed, sequence analysis of these products was more consistent with transposition into the termini of another transposon copy rather than the formation of an excised circular form (data not shown). Therefore, the frequency at which excised *SB* elements undergo circularization in mammalian cells appears to be extremely low, if it occurs at all. Although we are continuing to investigate the molecular basis for improved transposition in DNA-PK-deficient cells, these results suggest that transposon circularization by the NHEJ machinery is unlikely to play a major role in the regulation of DNA transposition in mammals.

TABLE 1. Plasmid-based transposition in normal and DNA-PK-deficient cell lines

Cell line	Genotype	No. of insertion events[a]		Transposition ratio[b]
		Active *SB*	Inactive *SB*	
HeLa	wt[c]	490 ± 53	9 ± 3	54
C-MHB-2	wt	910 ± 84	49 ± 7	19
S-MHB-2	DNA-PK$_{cs}^{-}$	720 ± 100	30 ± 20	24
CHO-K1	wt	430 ± 79	50 ± 5	9
xrs-5	Ku86^{-}	318 ± 117	24 ± 5	13
V79-4	wt	660 ± 31	89 ± 16	7
XR-V15B	Ku86^{-}	490 ± 7	34 ± 5	14

[a] The mean numbers of transposon insertion events in each cell line were determined as described in Materials and Methods and are based on three separate transfection experiments.
[b] The transposition ratio for each cell line is the mean number of *SB*-dependent integrants divided by the mean number of *SB*-independent integrants.
[c] wt, wild type.

Mammalian Ku protein is required for accurate DSB repair after *SB* element transposition. To determine whether NHEJ factors are involved in repairing the DSBs produced during transposon excision in mammalian cells, we studied the excision step of *SB* element transposition by PCR using Hirt DNA obtained from normal and Ku-deficient hamster cells following transfection with transposon-containing and transposase-encoding plasmids. In contrast to pCMV-mSB-transfected control cells, both normal and Ku-deficient cells were capable of supporting the production of an appropriately sized PCR product following expression of the wild-type transposase, although the amount of specific end-joining activity observed was significantly reduced in the absence of Ku compared to that for each of the controls (Fig. 4A). These results are consistent with transposase-mediated *SB* element excision and demonstrate that mammalian cells possess a Ku-independent end-joining activity that can process transposase-induced DSBs.

Based on the reduced recovery of the specific repair product in Ku-deficient cells, we tested whether these findings reflected a decrease in the overall rate of repair or whether there was a concomitant increase in recovery of alternatively sized prod-

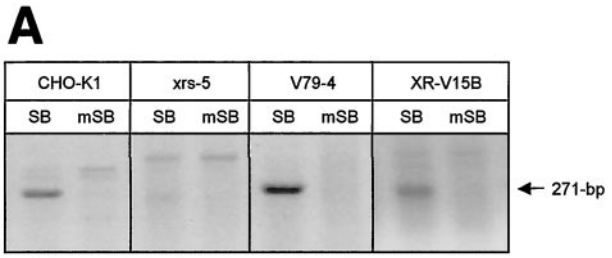

FIG. 4. Repair of transposase-induced DSBs in the presence and absence of mammalian Ku DNA end-binding activity. (A) Transposon excision and DSB repair in the presence and absence of Ku protein. Wild-type (CHO-K1 and V79-4) and Ku-deficient (*xrs-5* and XR-V15B) hamster cells were transfected with donor plasmid pTnori (containing a 3.4-kb *neo*-marked *SB* element) together with either pCMV-SB or pCMV-mSB. Hirt DNA was isolated 30 h later and analyzed by PCR for the presence of a 271-bp product of excision and repair. (B) Variety of DSB repair products produced in the presence and absence of mammalian Ku. Base pair deletions (dashes) in the region surrounding the excision site are shown. (C) Example of the homologous sequences present at the junctions between the broken DNA molecule and captured sequences. Shaded boxes, positions of microhomologies at each end of the junction and within the region where the two inserts are joined.

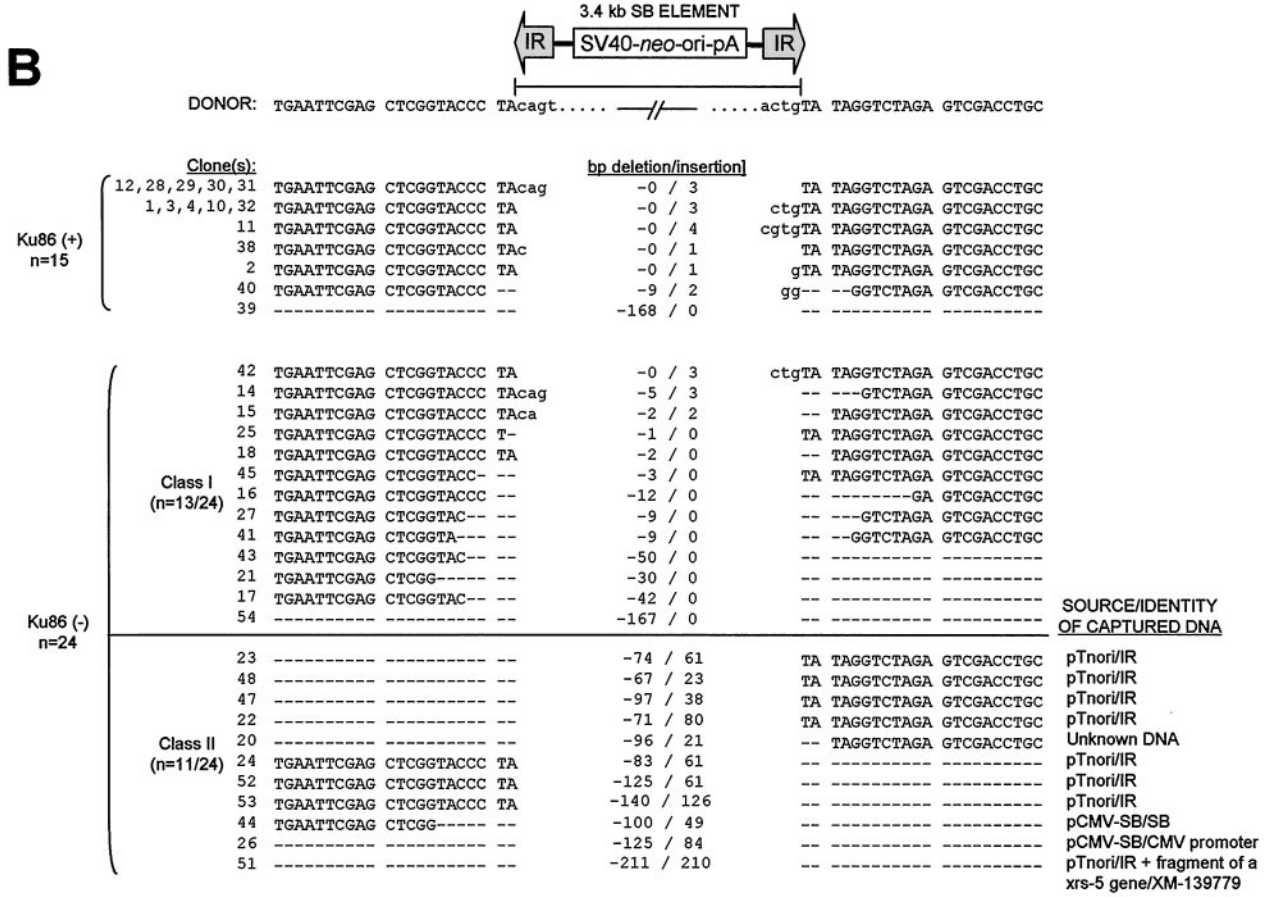

ucts in the absence of Ku. To do this, we cloned and sequenced the DNA contained within the 400-bp region surrounding the major repair products made in the presence and absence of Ku. In 10 of the 15 clones isolated from wild-type control cells, the footprint left behind after *SB* element excision consisted of the terminal 3 nucleotides from either end of the transposon flanked by a pair of TA dinucleotides (i.e., TA-C[A/G]T-TA; Fig. 4B). Of the remaining five clones, three had atypically sized 1- and 4-bp footprints, one had a large deletion of 168 bp, and one had a small 9-bp deletion with an addition of two nontemplated nucleotides. In contrast to these findings, nearly every DSB repair product isolated from two different Ku-deficient cell lines (XR-V15B and *xrs-5*) lacked any apparent footprint following *SB* element excision and frequently had large deletions of neighboring sequences (Fig. 4B). Furthermore, approximately one-half of these clones also contained

short patches (21 to 210 bp) of foreign DNA (Fig. 4B; class II). Among these clones, most displayed precise joining of foreign sequences at one end of the break and significant degradative loss of neighboring DNA (74 to 140 bp) at the other end. Using BLAST homology-based searches, we found that the majority of insertions corresponded to terminal portions of the transposon end sequences ($n = 7$), which is most consistent with a canonical homologous recombination event. However, two other clones (26 and 44) contained homologous portions of the transposase helper plasmid pCMV-SB, with approximately 6 to 8 bp of microhomology at their breakpoints. We also found one clone which contained a chimeric insert consisting of an internal portion of the transposon IR fused to portions of cellular DNA from a putative mouse pheromone receptor (clone 51; positivity, 88/104; GenBank accession no. XM-139779). In this clone, we also found evidence of microhomologies at each of the vector-DNA junctions (Fig. 4C). These three recombination events are highly consistent with microhomology-directed gap repair at the excision site. Therefore, Ku seems to function at the excision site during DNA transposition by preventing both degradation of the resulting 3′ overhangs and high-frequency recombination with ectopic DNA sequences. In this manner, mammalian Ku or DNA-PK or both play an important role in mediating the high-fidelity rejoining of transposase-induced DSBs in mammalian cells.

A reporter system for studying DSB repair following transposon excision from host cell chromosomes. We considered the possibility that the analysis of DNA repair using naked DNA might not adequately reflect repair of cellular DNA, which is known to rapidly associate with nuclear histone proteins to form chromatin. We therefore studied DNA repair following *SB* element excision from mammalian cell chromosomes using a positive-selection scheme that permits detection and analysis of rare chromosomal transposition events at random single-copy genetic loci (Fig. 5A). This strategy made use of a selectable excision reporter construct in which a hygromycin-marked *SB* transposon was inserted into a selectable neomycin marker cassette to inactivate its function. This entire reporter construct was incorporated into a lentivirus to facilitate its delivery to random genomic loci of host cells. Following stable transduction with this lentivirus-based vector and expression of the transposase in *trans*, movement of the nonautonomous *SB* element is triggered, resulting in reactivation of the neomycin resistance cassette. Therefore, this selection-based approach permits the rapid isolation of cells that have undergone genomic transposon excision and DSB repair.

Chromosomal transposition in normal and Ku-deficient cells. We studied cellular DSB repair following transposon mobilization in wild-type and NHEJ-defective mammalian cells. To do this, we stably transduced HeLa cells and Ku-deficient XR-V15B cells with the lentivirus-based excision reporter construct and screened clonal populations of transduced cells for resistance to hygromycin and sensitivity to G418. We then used Southern blot analyses to identify four G418-sensitive ($G418^S$) Hyg^R HeLa clones and eight $G418^S$ Hyg^R XR-V15B cell clones containing a single copy of the reporter construct at different genomic locations. These cell clones were expanded, transfected with plasmids encoding either the *SB* transposase or GFP as a control, and then placed under G418 selection to identify transposon excision events.

Whereas none of the reporter lines reverted to G418 resistance in the presence of GFP, we obtained a total of 28 $G418^R$ clones after transposase expression in the four HeLa-based reporter lines. This corresponded to an average of 5×10^{-6} transposition events per transfected HeLa cell (data not shown), which is equivalent to the frequency of chromosomal *SB* transposition observed previously at the *Hprt* locus in mouse embryonic stem cells (38). We characterized each $G418^R$ clone at the molecular level using a Southern blotting approach. Assuming high-fidelity repair following precise excision of the *SB* element, we could predict the postexcision structure in these $G418^R$ clones (Fig. 5A). Using a *neo*-specific probe, we detected the predicted 3.1-kb *Ava*I restriction fragment in 20 of 28 clones by Southern blot analysis (Fig. 5B), which is consistent with proper transposon excision from the neomycin resistance cassette. Interestingly, six of the remaining eight clones produced smaller *Ava*I fragments, ranging from 2.5 to 3.0 kb, whereas two clones exhibited a detectably larger 3.3-kb fragment. To further demonstrate that transposon loss occurred by a transposase-mediated process, we studied transposon reinsertion frequencies in $G418^R$ clones by both transposon-specific PCR (data not shown) and Southern blot analyses using the restriction enzyme *Spe*I, which cuts once within the Hyg^R transposon. Results demonstrate frequent reinsertion of elements into novel genomic loci, which is consistent with transposase-mediated element excision from the donor site (Fig. 5C). These were concordant with results obtained in expression-based studies in which we assayed for expression of transposed sequences by selection in hygromycin, although we identified at least two instances where the transposon jumped into transcriptionally inactive cellular DNA (Fig. 5B, clones 6-2 and 8-1). Taken together, these results suggest that cellular DSB repair after *SB* element transposition in NHEJ-proficient mammalian cells is generally precise but can sometimes result in significant deletion and/or addition of DNA sequences at the excision site.

In marked contrast to the HeLa-derived clones, none of the eight Ku-deficient reporter lines produced a single $G418^R$ colony following transposase expression. This result is perhaps not surprising considering the facts that (i) the frequency of *SB* chromosomal transposition observed in this study and elsewhere (38) was extremely low and (ii) the frequency of rejoining genomic DSBs is more than 100-fold lower in the absence of Ku (34). Whether the high-stringency selection-based approach used here precludes the recovery of most Ku-independent repair events, which often involve significant addition and/or deletion of DNA sequences, remains presently unclear. However, considering our earlier work showing efficient *SB* transposition in Ku-deficient cells, we propose that Ku is likely essential for efficient and proper rejoining of genomic transposase-induced DSBs.

Transposon excision from HeLa cell chromosomes results in frequent and extensive loss of flanking cellular DNA. We amplified a fragment encompassing the excision site from each of the HeLa-derived $G418^R$ clones by PCR and sequenced it. In comparison to clones derived from various wild-type mouse cells, those isolated from wild-type human cells in which DSB repair events occurred exhibited a wider diversity of 1- to 3-bp footprints after *SB* element excision, as well as a much higher frequency of DNA loss in the regions surrounding the excision

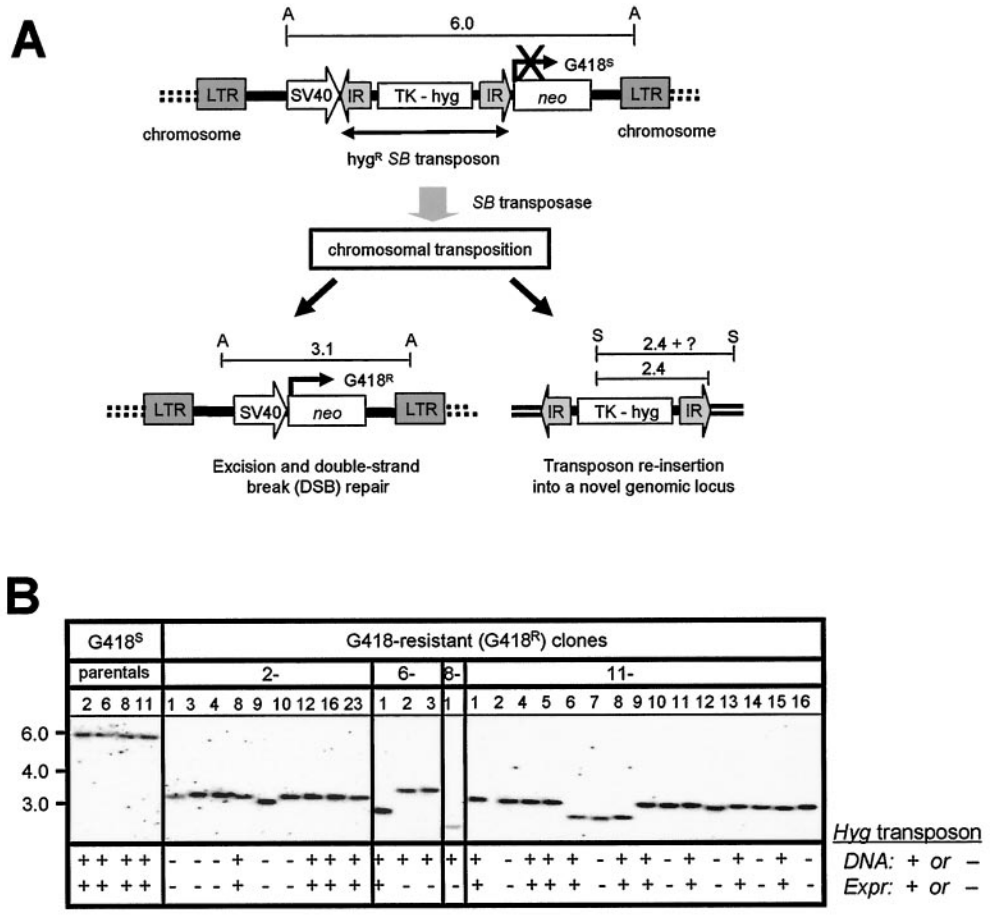

site. Deletions of flanking regions ranged in size from as little as 2 bp to as much as 610 bp and sometimes extended into the neighboring simian virus 40 promoter (Fig. 6A, clones 11-7 and 8-1). The isolation of these clones suggests that the upstream retroviral long terminal repeat promoter can sometimes compensate for progressive DNA degradation after *SB* element excision. Interestingly, we could identify 1 to 7 bp of microhomology at the junctions of clones which had undergone large deletion of flanking sequences ($n = 6$; Fig. 6B, top), suggesting a role for microhomology-dependent strand annealing in the repair of transposase-induced DNA lesions. Furthermore, the one clone which was found to contain a 235-bp LINE-1 (L1MB7-type) retrotransposon insertion from chro-

FIG. 5. Chromosomal excision and reinsertion of a nonautonomous *SB* element in HeLa cells. (A) Genetic-selection strategy to study DSB repair following rare transposon excision from random chromosomal loci. A neomycin resistance (*neo*) gene under the control of the simian virus 40 (SV40) promoter is inactivated by the insertion of a nonautonomous *SB* element containing the Hyg^R gene driven by the thymidine kinase (TK) promoter. Upon packaging into a lentivirus vector, this excision testing construct randomly integrates as a single-copy provirus into the genomes of infected cells. Following transient expression of the *SB* transposase, the *SB* element is excised and expression of the *neo* gene is activated, resulting in resistance to the drug G418. In some instances, the excised hygromycin resistance *SB* element reintegrates into the genome and acquires novel flanking sequences. Shown are the predicted structures of the testing construct, with approximate distances in kilobases between flanking *Ava*I (A) and *Spe*I (S) sites, before (top) and after (bottom) *SB*-mediated transposon excision. LTR, HIV-1 long terminal repeat. (B) Southern blot analysis confirms excision of the *SB* element from the testing construct. Twenty micrograms of total DNA from all $G418^R$ colonies, as well as the four $G418^S$ parental clones, was digested with *Ava*I, separated by ethidium bromide gel electrophoresis, transferred to nitrocellulose, and then hybridized to a *neo* probe. The molecular marker (kilobases) is shown to the left. The presence (+) and absence (−) of an expressible transposon in each clone was investigated by both PCR and hygromycin-dependent growth selection. (C) Genomic reintegration of the transposon into novel chromosomal loci following *SB*-mediated excision. Twenty micrograms of total DNA from each $G418^S$ parental clone and 13 of the resulting Hyg^R $G418^R$ clones was digested with *Spe*I (cuts once in the transposon), separated by ethidium bromide gel electrophoresis, transferred to nitrocellulose, and then hybridized to a ^{32}P-radiolabeled hygromycin fragment.

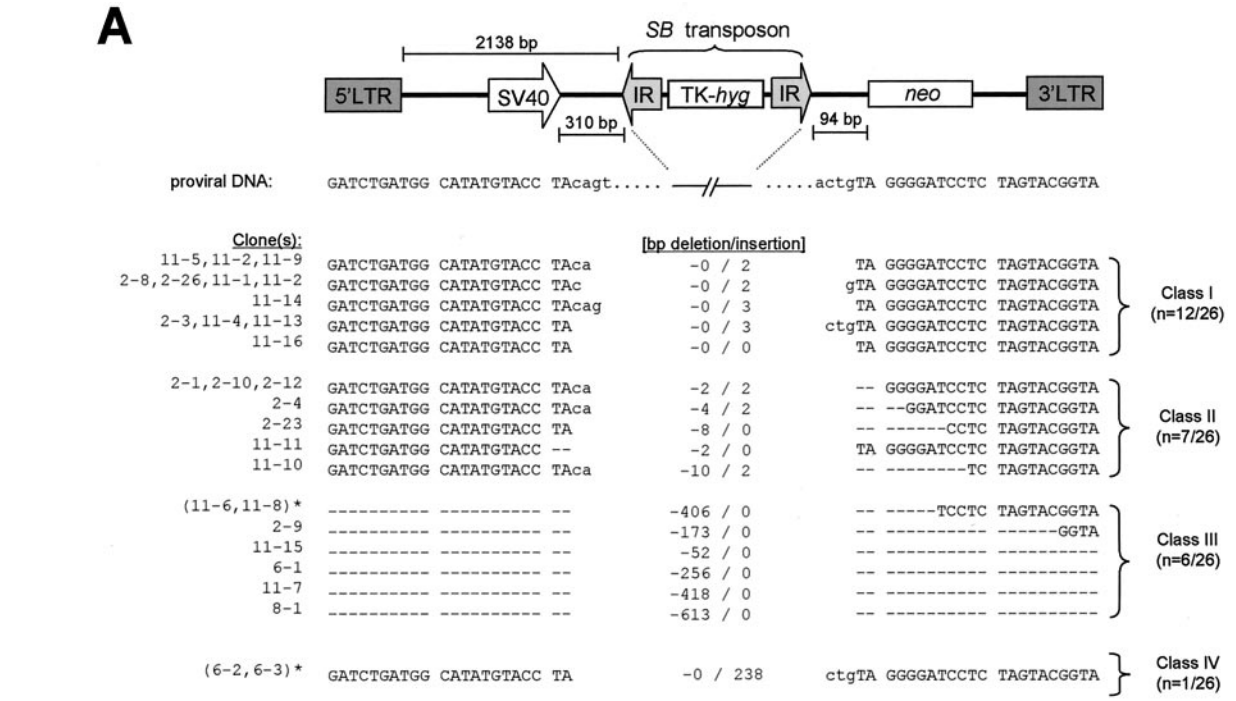

FIG. 6. Rejoining of cellular transposase-induced DSBs in wild-type human cells. (A) DNA sequence analysis of the donor sites after excision of the *SB* element from the testing construct located at four different genomic loci. All examples of recovered excision products are shown together with the original parental sequence. Footprints are in lowercase. Dashes, deleted nucleotides; asterisks, duplicate clones. (B) Microhomology at junctions of repaired genomic DNA breaks in class III G418^R clones. Columns A and B show the nucleotides at the edges of the DNA fragment lost during transposon excision and DSB repair in each clone. The shaded regions in columns A and B represent deleted sequences with homology to the right and left junctions of the G418^R provirus, respectively. The presence of microhomologies at one end of a clone that acquired a retrotransposon insert is shown below.

mosome X (clone 6-2; positivity, 241/242; GenBank accession no.AC097259) also contained a 6-bp stretch of homologous sequence at one end, suggesting that recombination with ectopic sequences can also occur in wild-type cells (Fig. 6B, bottom). Taken together, these data suggest that significant loss and/or addition of cellular DNA can occur in human cells after *SB* element transposition.

DISCUSSION

Herein, we have studied how mammalian cells respond to the DNA-damaging activity of the eukaryotic transposable element *SB*. Using plasmid- and chromosome-based reporter systems, we have shown that components of the DNA-PK complex are required for high-fidelity DNA repair after *SB* element excision in both cultured mammalian cells and in vivo in mouse somatic tissues. Nevertheless, we found that mammalian cells lacking Ku DNA end-binding activity could still process transposase-induced DSB but did so by more-error-prone pathways, which resulted in extensive deletion of free ends and recombination with ectopic templates (Fig. 7). Therefore, the DNA-PK-dependent NHEJ pathway is involved in preserving genomic integrity during DNA transposition in mammalian cells.

In recent years, there have been a number of investigations of *SB* element activity which included the isolation of excision site end-joining products from various cell types. Although DSB repair after *SB* transposition in zebra fish embryos (13), mouse embryonic stem cells (38), and transgenic mouse somatic tissues (21) produced 3-bp footprints corresponding to transposon end sequences, repair in mouse spermatids favored 1- and 2-bp footprints (16). Similarly, different-size footprints were observed after Tc3 transposition in zebra fish and *Caenorhabditis elegans* (52, 63), as well as with *Minos* in *Drosophila melanogaster* and mice (3, 68). One likely explanation for these structural differences involves cell type-dependent variation in the activity of a critical host factor involved in repair after

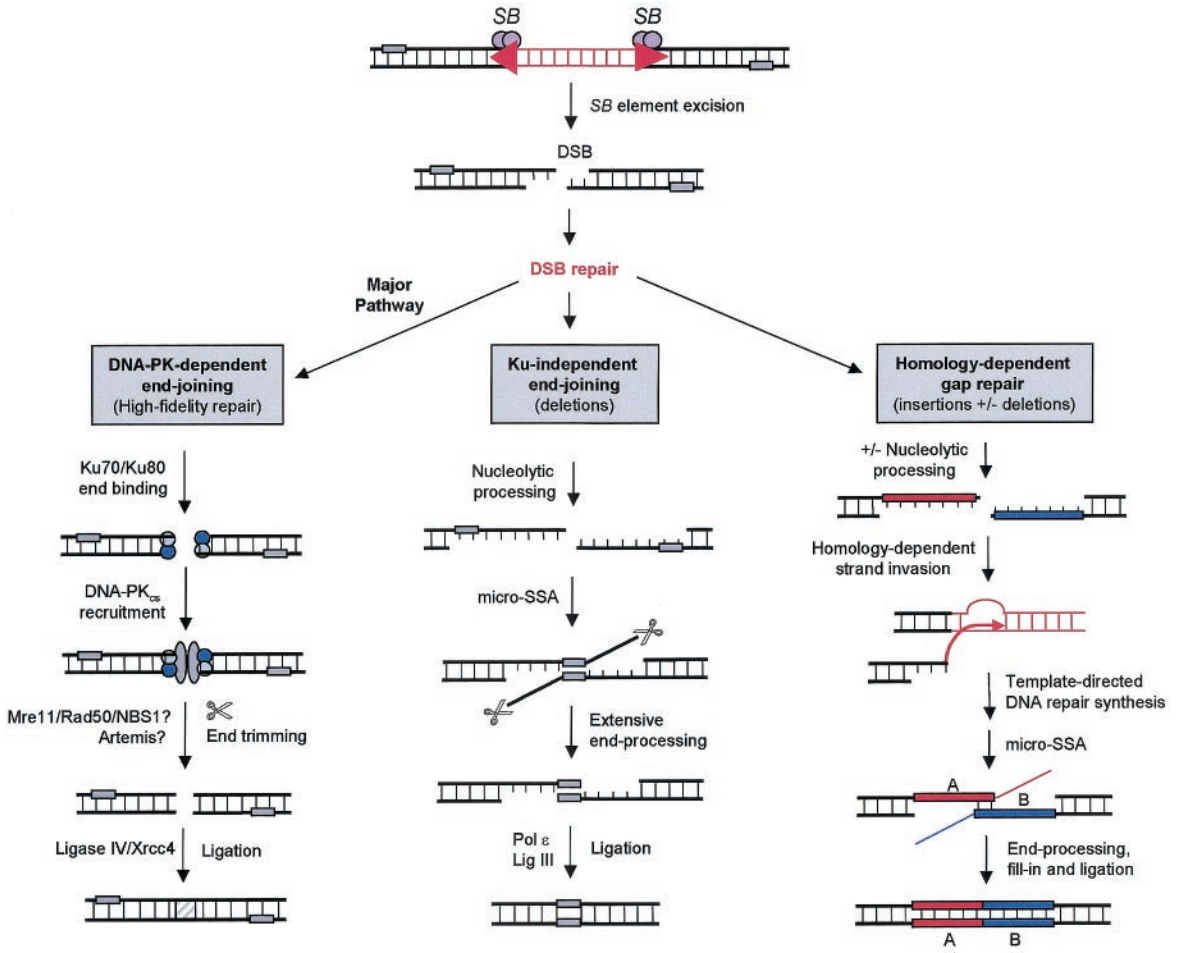

FIG. 7. Multiple pathways for DNA repair after *SB* element excision in mammalian cells. The majority of DSBs introduced during *SB* element excision are repaired by a DNA-PK-dependent NHEJ pathway which involves the binding of Ku heterodimers to free DNA ends and subsequent recruitment of DNA-PK$_{cs}$. DNA ends are then unwound and processed, possibly by Artemis or the MRN complex, and then ligated by the DNA ligase IV/XRCC4 complex. In the absence of DNA-PK activity, at least two different Ku-independent repair pathways are activated to fill the DNA gap. The first is a poorly defined error-prone NHEJ pathway that processes DSBs by illegitimate pairing of distant regions of microhomology (small shaded rectangles), followed by ligation and deletion of the intervening DNA sequence. The second route involves strand invasion of DNA sources with homology, which results in the insertion of a short DNA segment at the break site. micro-SSA, microhomology-dependent single-strand annealing.

transposon excision. In support of this notion, we observed a clear and dramatic shift away from the major 3-bp footprint within three different cell types (hamster ovary, hamster lung, and mouse liver) whenever components of the DNA-PK were disrupted by genetic mutation. For instance, as little as 4% (1 of 23) of the footprints recovered from DNA-PK$_{cs}$-deficient *scid* mice contained the major 3-bp footprint, compared to 87% (20 of 23) from genetically matched wild-type mice. These data strongly suggest that the Ku/DNA-PK$_{cs}$ complex plays a vital role in controlling excision site junctional diversity following transposon mobilization in mammalian cells.

Our work suggests that, prior to ligation by the DNA ligase IV/XRCC4 complex, the Ku/DNA-PK$_{cs}$ complex limits processing of the free DNA ends produced during *SB* element transposition in mammalian cells. Interestingly, Ku is also known to bind the termini of the *P* element and to protect the *P* element ends when transposition creates a double-strand gap in *Drosophila* (5, 58). Taken together, these results suggest that DNA-PK activity provides a function necessary for transpositional recombination in eukaryotes.

Although the identities of other NHEJ factors involved in DNA transposition remain poorly defined, the production of DSBs with incompatible 3′overhangs during *SB* element excision strongly suggests the involvement of a nuclease that can process these ends to facilitate efficient rejoining. Potential factors involved in this end-processing step could include Artemis (39) or possibly the MRN complex (60). Indeed, recent studies in our laboratory suggest that inhibiting the MRN complex can dramatically impair *SB* element-induced DSB repair (S. Yant, unpublished data). Alternatively, it is possible that *SB* transposase activity itself facilitates the processing of the broken DNA molecule. Indeed, the closely related RAG1/RAG2 recombinase and Tn*10* transposase both possess 3′ flap endonuclease activity (56). Whether *SB* is capable of performing an analogous function is uncertain. Future studies into these and other related issues will likely require the development of an in

vitro transposition system for *SB*, which does not currently exist.

Studies of mammalian cells with the rare restriction endonuclease I-*Sce*I have shown that, although the vast majority of end-joining reactions are relatively accurate, a small minority of DSBs in normal cells can be processed by an error-prone NHEJ pathway (15). This repair route can function independent of Ku and appears to involve the joining of DNA ends at regions of microhomology (1 to 4 bp), resulting in deletion of the intervening sequence (46). Our work described herein suggests that DNA-PK-independent pathways contribute to inaccurate repair during DNA transposition in mammals. Although most of the factors responsible for this error-prone end-joining activity remain poorly defined, a recent study has implicated BRCA1, which associates with the MRN complex, in microhomology-mediated end joining (70). In addition, in vitro studies have also identified DNA polymerase ε (pol ϵ), DNA ligase III, and exonuclease activities of 5′-3′ and 3′-5′ directionalities in these processes (19). Finally, a role for Mre11 and poly(ADP-ribose) polymerase-1 in DNA-PK_{cs}-independent V(D)J recombination was recently shown (7). Future studies will thus be necessary to elucidate whether any of these alternative end-joining factors is involved in DSB repair after DNA transposition in mammalian cells.

Our studies of Ku-deficient cells suggest that mammalian cells can also remove transposase-induced DSBs by coupling conventional end joining with an error-prone homologous recombination pathway. These repair events involved insertions of ectopic DNA templates with homologous sequences and had properties consistent with aberrant end joining after aborted homologous recombination. Similarly, transposon excision in both flies (2, 17, 37, 43) and worms (47, 49) also triggers recombination with ectopic templates, resulting in the introduction of new sequences into the original donor site. Whether the events that we observed in mammalian cells involve the major RAD52 group proteins or other factors recently implicated in homologous recombination (61, 62), such as ATM (ataxia telangiectasia mutated), ATR (Rad3-related kinase), BRCA-1, BRCA-2, WRN, and BLM, is not yet known. However, since most of the insertions we recovered contained transposon DNA with at least one intact *SB* binding site, it is possible that the utilization of this repair pathway in nature contributed to the inactivation of these and other transposable elements (36).

Following transposase-mediated excision, the newly excised *SB* element must reinsert into a new target site in order to complete a full cycle of transposition. Our data suggest that cell lines deficient in DNA-PK activity support ~1.6-fold more transposon insertions than parental wild-type cells. Interestingly, Baekelandt et al. also observed more-efficient lentivirus transduction in DNA-PK-deficient cells and in *scid* mouse brain than in infected controls, but only at low virus titers (<1 transducing unit/cell) (4). At higher virus titers, significant cytotoxicity was observed, prompting the notion that DNA-PK serves a protective role during excessive retrovirus integration (4). Importantly, irrespective of the presence or absence of DNA-PK_{cs}, we did not observe any evidence for transposition-dependent cell death either in cell culture or in vivo in mice (S. Yant, unpublished data). These findings could suggest that the levels of *SB* element transposition in mammalian cells may be low enough to prevent initiation of a cell death response. Alternatively, it may be that the double-stranded ends of excised elements are actively removed by NHEJ factors via direct end-to-end joining. Although a recent report has indeed described a role for DNA-PK in the circularization of unintegrated retrovirus cDNA genomes (33), our data do not support an obvious role for NHEJ in the processing of *SB* elements after transposase-mediated excision. These findings could be readily explained if *SB* transposition involved the formation of a DNA hairpin intermediate at the transposon termini. Although hairpin formation is involved in V(D)J joining (40) and the excision of many transposable elements (6, 27, 64), this process does not appear to occur during transposition of Tc1/*mariner*-like elements (12). Alternatively, these results might reflect the involvement of a highly stable protein-DNA complex at the transposon termini. Such a complex could prevent reactions with cellular NHEJ factors that might otherwise diminish *SB* transposition efficiencies and could theoretically prevent the cell from mounting an apoptosis-inducing DNA damage response against the double-stranded ends of the excised element.

At any given time, cells deficient in DNA-PK end-joining activity are likely to contain more overall DNA damage, including DSBs, than NHEJ-proficient cells. Therefore, it is conceivable that improved transposon insertion frequencies in DNA-PK-deficient cells may originate from an inherent tendency for *SB* elements to insert into sites of chromosomal damage. Indeed, recent experiments utilizing the mammalian LINE-1 retrotransposon suggest that at least some transposable elements can target DSBs to facilitate repair (42). If this were true for *SB* elements, then such insertions into noncanonical target sites would lack flanking TA dinucleotides (Fig. 1). However, recent analysis of insertion sites from Ku86-deficient cells showed flanking TA sequences in every case examined ($n = 11$; S. Yant, unpublished data), suggesting that transposase-mediated insertion into endogenous DSBs may be an unlikely mechanism. Alternatively, *SB* elements may exhibit a targeting preference similar to that of the bacterial transposon Tn*7*, which preferentially transposes into regions proximal to DNA DSBs rather than the breaks themselves (45). Although we favor the latter hypothesis, additional studies will be necessary to further clarify this important issue.

As with retrovirus DNA integration, DNA transposition proceeds through a series of DNA-cutting and -joining reactions that produces an integration intermediate containing single-strand gaps in the host DNA. These gaps must be filled, and the 5′ ends of the transposon must be joined to the host DNA. Although the DNA-PK complex is known to be important for joining DSBs, it is not thought to be involved in the covalent chemistry of gap repair. Therefore, a report by Daniel et al. (11) claiming an essential role for DNA-PK during retrovirus integration engendered considerable interest at the time it was published (2000). This claim was based on the observation that retrovirus transduction was reduced in murine *scid* cells and was accompanied by cell death due to apoptosis (10, 11). Based on the structural and functional similarities between retroviral integrases and the *SB* transposase (50), it seemed reasonable that DNA-PK might play an essential role in *SB* element integration as well. However, our analysis of *SB*

transposition in cultured mammalian cells and in vivo in adult mice shows quite clearly that DNA-PK is not required for gap repair after transposase-mediated integration.

DNA repair pathways such as base excision repair and mismatch repair involve related gap repair steps (29). Although pol β plays a major role in sealing the gaps during base excision repair, recent analysis of *SB* element transposition in pol β-deficient cells argues against an essential role for this repair factor in transposon insertion (S. Yant, unpublished data). However, since pol δ and its cofactor PCNA can also support base excision repair (29), these results likely reflect a redundancy among the components of gap repair pathways. In support of this hypothesis, in vitro studies by Yoder and Bushman have shown that several host polymerases and ligases can act together to repair the gapped DNA structure produced during retrovirus integration (67). Furthermore, although there have been conflicting reports regarding the ability of retroviral integrase to carry out gap repair through an intrinsic DNA polymerase activity (1, 67), these studies raise important questions regarding what role, if any, the *SB* transposase plays in the DNA damage response to *SB* element transposition. Finally, successful completion of the retroviral integration process was recently shown to depend on the activity of ATM and ATR (9). Future studies into these and other protein factors should help clarify the steps involved in completing transposon integration in mammalian cells.

Irrespective of which proteins are actually involved in these processes, these factors must first gain access to the gaps in integration intermediates in order for repair to take place. Following DNA cleavage at the excision site, the *SB* transposase is generally thought to stably associate with the transposon termini, suggesting that it may need to be actively removed from integration intermediates in mammalian cells. Studies with the MuA transposase indicate that this protein must be removed by the action of the ClpX chaperone in an ATP-dependent fashion to permit completion of Mu transposition (31, 32). Since a similar process has also been proposed for retroviral integrase (67), investigations into the requirement for active transposase disassembly during *SB* transposition seem warranted.

In summary, we have characterized the major DNA repair pathways involved in the damage response to transposon mobilization in mammalian cells. In the process, we have established a major role for the DNA-PK complex in removing the DNA damage produced during *SB* element transposition and have identified DNA transposition as an alternative new tool for studying mammalian DNA repair. Continued work in this field should help fully clarify the different molecular pathways that remove transposase-inflicted DNA damage in mammals, as well as determine how the utilization of these pathways may vary during different stages of the cell cycle and/or development. Finally, since our data suggest that *SB* element excision can produce a hot spot for recombination in mammalian cells, additional work may shed further light on the ongoing process of eukaryotic genome evolution and may ultimately provide insight into the origin of genetic diseases (53) and cancers associated with genetic instability.

ACKNOWLEDGMENTS

We thank L. Meuse for his excellent technical assistance, H. Nakai for many helpful discussions, and J. Mikkelsen for critical reading of the manuscript.

This work was supported by NIH grant AR44012 (M.A.K.).

REFERENCES

1. **Acel, A., B. E. Udashkin, M. A. Wainberg, and E. A. Faust.** 1998. Efficient gap repair catalyzed in vitro by an intrinsic DNA polymerase activity of human immunodeficiency virus type 1 integrase. J. Virol. **72:**2062–2071.
2. **Adams, M. D., M. McVey, and J. J. Sekelsky.** 2003. *Drosophila* BLM in double-strand break repair by synthesis-dependent strand annealing. Science **299:**265–267.
3. **Arca, B., S. Zabalou, T. G. Loukeris, and C. Savakis.** 1997. Mobilization of a Minos transposon in *Drosophila melanogaster* chromosomes and chromatid repair by heteroduplex formation. Genetics **145:**267–279.
4. **Baekelandt, V., A. Claeys, P. Cherepanov, E. De Clercq, B. De Strooper, B. Nuttin, and Z. Debyser.** 2000. DNA-dependent protein kinase is not required for efficient lentivirus integration. J. Virol. **74:**11278–11285.
5. **Beall, E. L., A. Admon, and D. C. Rio.** 1994. A *Drosophila* protein homologous to the human p70 Ku autoimmune antigen interacts with the P transposable element inverted repeats. Proc. Natl. Acad. Sci. USA **91:**12681–12685.
6. **Bhasin, A., I. Y. Goryshin, and W. S. Reznikoff.** 1999. Hairpin formation in Tn*5* transposition. J. Biol. Chem. **274:**37021–37029.
7. **Brown, M. L., D. Franco, A. Burkle, and Y. Chang.** 2002. Role of poly(ADP-ribosyl)ation in DNA-PKcs-independent V(D)J recombination. Proc. Natl. Acad. Sci. USA **99:**4532–4537.
8. **Chen, L., K. Trujillo, W. Ramos, P. Sung, and A. E. Tomkinson.** 2001. Promotion of Dnl4-catalyzed DNA end-joining by the Rad50/Mre11/Xrs2 and Hdf1/Hdf2 complexes. Mol. Cell **8:**1105–1115.
9. **Daniel, R., G. Kao, K. Taganov, J. G. Greger, O. Favorova, G. Merkel, T. J. Yen, R. A. Katz, and A. M. Skalka.** 2003. Evidence that the retroviral DNA integration process triggers an ATR-dependent DNA damage response. Proc. Natl. Acad. Sci. USA **100:**4778–4783.
10. **Daniel, R., R. A. Katz, G. Merkel, J. C. Hittle, T. J. Yen, and A. M. Skalka.** 2001. Wortmannin potentiates integrase-mediated killing of lymphocytes and reduces the efficiency of stable transduction by retroviruses. Mol. Cell. Biol. **21:**1164–1172. (Erratum, **21:**2617.)
11. **Daniel, R., R. A. Katz, and A. M. Skalka.** 1999. A role for DNA-PK in retroviral DNA integration. Science **284:**644–647.
12. **Dawson, A., and D. J. Finnegan.** 2003. Excision of the *Drosophila* mariner transposon *Mos*I. Comparison with bacterial transposition and V(D)J recombination. Mol. Cell **11:**225–235.
13. **Dupuy, A. J., K. Clark, C. M. Carlson, S. Fritz, A. E. Davidson, K. M. Markley, K. Finley, C. F. Fletcher, S. C. Ekker, P. B. Hackett, S. Horn, and D. A. Largaespada.** 2002. Mammalian germ-line transgenesis by transposition. Proc. Natl. Acad. Sci. USA **99:**4495–4499.
14. **Dupuy, A. J., S. Fritz, and D. A. Largaespada.** 2001. Transposition and gene disruption in the male germline of the mouse. Genes. J. Genet. Dev. **30:**82–88.
15. **Feldmann, E., V. Schmiemann, W. Goedecke, S. Reichenberger, and P. Pfeiffer.** 2000. DNA double-strand break repair in cell-free extracts from Ku80-deficient cells: implications for Ku serving as an alignment factor in non-homologous DNA end joining. Nucleic Acids Res. **28:**2585–2596.
16. **Fischer, S. E., E. Wienholds, and R. H. Plasterk.** 2001. Regulated transposition of a fish transposon in the mouse germ line. Proc. Natl. Acad. Sci. USA **98:**6759–6764.
17. **Gloor, G. B., N. A. Nassif, D. M. Johnson-Schlitz, C. R. Preston, and W. R. Engels.** 1991. Targeted gene replacement in *Drosophila* via P element-induced gap repair. Science **253:**1110–1117.
18. **Gorbunova, V., and A. A. Levy.** 1997. Circularized Ac/Ds transposons: formation, structure and fate. Genetics **145:**1161–1169.
19. **Gottlich, B., S. Reichenberger, E. Feldmann, and P. Pfeiffer.** 1998. Rejoining of DNA double-strand breaks in vitro by single-strand annealing. Eur. J. Biochem. **258:**387–395.
20. **Hammarsten, O., and G. Chu.** 1998. DNA-dependent protein kinase: DNA binding and activation in the absence of Ku. Proc. Natl. Acad. Sci. USA **95:**525–530.
21. **Horie, K., A. Kuroiwa, M. Ikawa, M. Okabe, G. Kondoh, Y. Matsuda, and J. Takeda.** 2001. Efficient chromosomal transposition of a Tc1/mariner-like transposon Sleeping Beauty in mice. Proc. Natl. Acad. Sci. USA **98:**9191–9196.
22. **Huang, J., and W. S. Dynan.** 2002. Reconstitution of the mammalian DNA double-strand break end-joining reaction reveals a requirement for an Mre11/Rad50/NBS1-containing fraction. Nucleic Acids Res. **30:**667–674.
23. **Ivics, Z., P. B. Hackett, R. H. Plasterk, and Z. Izsvak.** 1997. Molecular reconstruction of Sleeping Beauty, a Tc1-like transposon from fish, and its transposition in human cells. Cell **91:**501–510.
24. **Izsvak, Z., Z. Ivics, and R. H. Plasterk.** 2000. Sleeping Beauty, a wide

host-range transposon vector for genetic transformation in vertebrates. J. Mol. Biol. **302:**93–102.
25. **Izsvak, Z., D. Khare, J. Behlke, U. Heinemann, R. H. Plasterk, and Z. Ivics.** 2002. Involvement of a bifunctional, paired-like DNA-binding domain and a transpositional enhancer in Sleeping Beauty transposition. J. Biol. Chem. **277:**34581–34588.
26. **Kay, M. A., F. Graham, F. Leland, and S. L. Woo.** 1995. Therapeutic serum concentrations of human alpha-1-antitrypsin after adenoviral-mediated gene transfer into mouse hepatocytes. Hepatology **21:**815–819.
27. **Kennedy, A. K., A. Guhathakurta, N. Kleckner, and D. B. Haniford.** 1998. Tn*10* transposition via a DNA hairpin intermediate. Cell **95:**125–134.
28. **Khanna, K. K., and S. P. Jackson.** 2001. DNA double-strand breaks: signaling, repair and the cancer connection. Nat. Genet. **27:**247–254.
29. **Klungland, A., and T. Lindahl.** 1997. Second pathway for completion of human DNA base excision-repair: reconstitution with purified proteins and requirement for DNase IV (FEN1). EMBO J. **16:**3341–3348.
30. **Labhart, P.** 1999. Nonhomologous DNA end joining in cell-free systems. Eur. J. Biochem. **265:**849–861.
31. **Levchenko, I., L. Luo, and T. A. Baker.** 1995. Disassembly of the Mu transposase tetramer by the ClpX chaperone. Genes Dev. **9:**2399–2408.
32. **Levchenko, I., M. Yamauchi, and T. A. Baker.** 1997. ClpX and MuB interact with overlapping regions of Mu transposase: implications for control of the transposition pathway. Genes Dev. **11:**1561–1572.
33. **Li, L., J. M. Olvera, K. E. Yoder, R. S. Mitchell, S. L. Butler, M. Lieber, S. L. Martin, and F. D. Bushman.** 2001. Role of the non-homologous DNA end joining pathway in the early steps of retroviral infection. EMBO J. **20:**3272–3281.
34. **Liang, F., P. J. Romanienko, D. T. Weaver, P. A. Jeggo, and M. Jasin.** 1996. Chromosomal double-strand break repair in Ku80-deficient cells. Proc. Natl. Acad. Sci. USA **93:**8929–8933.
35. **Liu, F., Y. Song, and D. Liu.** 1999. Hydrodynamics-based transfection in animals by systemic administration of plasmid DNA. Gene Ther. **6:**1258–1266.
36. **Lohe, A. R., E. N. Moriyama, D. A. Lidholm, and D. L. Hartl.** 1995. Horizontal transmission, vertical inactivation, and stochastic loss of mariner-like transposable elements. Mol. Biol. Evol. **12:**62–72.
37. **Lohe, A. R., C. Timmons, I. Beerman, E. R. Lozovskaya, and D. L. Hartl.** 2000. Self-inflicted wounds, template-directed gap repair and a recombination hotspot. Effects of the mariner transposase. Genetics **154:**647–656.
38. **Luo, G., Z. Ivics, Z. Izsvak, and A. Bradley.** 1998. Chromosomal transposition of a Tc1/mariner-like element in mouse embryonic stem cells. Proc. Natl. Acad. Sci. USA **95:**10769–10773.
39. **Ma, Y., U. Pannicke, K. Schwarz, and M. R. Lieber.** 2002. Hairpin opening and overhang processing by an Artemis/DNA-dependent protein kinase complex in nonhomologous end joining and V(D)J. recombination. Cell **108:**781–794.
40. **McBlane, J. F., D. C. van Gent, D. A. Ramsden, C. Romeo, C. A. Cuomo, M. Gellert, and M. A. Oettinger.** 1995. Cleavage at a V(D)J recombination signal requires only RAG1 and RAG2 proteins and occurs in two steps. Cell **83:**387–395.
41. **Montini, E., P. K. Held, M. Noll, N. Morcinek, M. Al-Dhalimy, M. Finegold, S. R. Yant, M. A. Kay, and M. Grompe.** 2002. In vivo correction of murine tyrosinemia type I by DNA-mediated transposition. Mol. Ther. **6:**759–769.
42. **Morrish, T. A., N. Gilbert, J. S. Myers, B. J. Vincent, T. D. Stamato, G. E. Taccioli, M. A. Batzer, and J. V. Moran.** 2002. DNA repair mediated by endonuclease-independent LINE-1 retrotransposition. Nat. Genet. **31:**159–165.
43. **Nassif, N., J. Penney, S. Pal, W. R. Engels, and G. B. Gloor.** 1994. Efficient copying of nonhomologous sequences from ectopic sites via P-element-induced gap repair. Mol. Cell. Biol. **14:**1613–1625.
44. **Park, F., K. Ohashi, W. Chiu, L. Naldini, and M. A. Kay.** 2000. Efficient lentiviral transduction of liver requires cell cycling in vivo. Nat. Genet. **24:**49–52.
45. **Peters, J. E., and N. L. Craig.** 2000. Tn*7* transposes proximal to DNA double-strand breaks and into regions where chromosomal DNA replication terminates. Mol. Cell **6:**573–582.
46. **Pfeiffer, P., W. Goedecke, and G. Obe.** 2000. Mechanisms of DNA double-strand break repair and their potential to induce chromosomal aberrations. Mutagenesis **15:**289–302.
47. **Plasterk, R. H.** 1991. The origin of footprints of the Tc1 transposon of *Caenorhabditis elegans*. EMBO J. **10:**1919–1925.
48. **Plasterk, R. H.** 1996. The Tc1/mariner transposon family. Curr. Top. Microbiol. Immunol. **204:**125–143.
49. **Plasterk, R. H., and J. T. Groenen.** 1992. Targeted alterations of the *Caenorhabditis elegans* genome by transgene instructed DNA double strand break repair following Tc1 excision. EMBO J. **11:**287–290.
50. **Plasterk, R. H., Z. Izsvak, and Z. Ivics.** 1999. Resident aliens: the Tc1/mariner superfamily of transposable elements. Trends Genet. **15:**326–332.
51. **Pluth, J. M., L. M. Fried, and C. U. Kirchgessner.** 2001. Severe combined immunodeficient cells expressing mutant hRAD54 exhibit a marked DNA double-strand break repair and error-prone chromosome repair defect. Cancer Res. **61:**2649–2655.
52. **Raz, E., H. G. van Luenen, B. Schaerringer, R. H. Plasterk, and W. Driever.** 1998. Transposition of the nematode *Caenorhabditis elegans* Tc3 element in the zebrafish *Danio rerio*. Curr. Biol. **8:**82–88.
53. **Reiter, L. T., T. Murakami, T. Koeuth, L. Pentao, D. M. Muzny, R. A. Gibbs, and J. R. Lupski.** 1996. A recombination hotspot responsible for two inherited peripheral neuropathies is located near a mariner transposon-like element. Nat. Genet. **12:**288–297. (Erratum, **19:**303, 1998.)
54. **Rose, A. M., and T. P. Snutch.** 1984. Isolation of the closed circular form of the transposable element Tc1 in *Caenorhabditis elegans*. Nature **311:**485–486.
55. **Ruan, K., and S. W. Emmons.** 1984. Extrachromosomal copies of transposon Tc*1* in the nematode *Caenorhabditis elegans*. Proc. Natl. Acad. Sci. USA **81:**4018–4022.
56. **Santagata, S., E. Besmer, A. Villa, F. Bozzi, J. S. Allingham, C. Sobacchi, D. B. Haniford, P. Vezzoni, M. C. Nussenzweig, Z. Q. Pan, and P. Cortes.** 1999. The RAG1/RAG2 complex constitutes a 3′ flap endonuclease: implications for junctional diversity in V(D)J and transpositional recombination. Mol. Cell **4:**935–947.
57. **Sekiguchi, J. M., Y. Gao, Y. Gu, K. Frank, Y. Sun, J. Chaudhuri, C. Zhu, H. L. Cheng, J. Manis, D. Ferguson, L. Davidson, M. E. Greenberg, and F. W. Alt.** 1999. Nonhomologous end-joining proteins are required for V(D)J recombination, normal growth, and neurogenesis. Cold Spring Harbor Symp. Quant. Biol. **64:**169–181.
58. **Staveley, B. E., T. R. Heslip, R. B. Hodgetts, and J. B. Bell.** 1995. Protected P-element termini suggest a role for inverted-repeat-binding protein in transposase-induced gap repair in *Drosophila melanogaster*. Genetics **139:**1321–1329.
59. **Sundaresan, V., and M. Freeling.** 1987. An extrachromosomal form of the Mu transposons of maize. Proc. Natl. Acad. Sci. USA **84:**4924–4928.
60. **Trujillo, K. M., S. S. Yuan, E. Y. Lee, and P. Sung.** 1998. Nuclease activities in a complex of human recombination and DNA repair factors Rad50, Mre11, and p95. J. Biol. Chem. **273:**21447–21450.
61. **Tutt, A., D. Bertwistle, J. Valentine, A. Gabriel, S. Swift, G. Ross, C. Griffin, J. Thacker, and A. Ashworth.** 2001. Mutation in Brca2 stimulates error-prone homology-directed repair of DNA double-strand breaks occurring between repeated sequences. EMBO J. **20:**4704–4716.
62. **van Gent, D. C., J. H. Hoeijmakers, and R. Kanaar.** 2001. Chromosomal stability and the DNA double-stranded break connection. Nat. Rev. Genet. **2:**196–206.
63. **van Luenen, H. G., S. D. Colloms, and R. H. Plasterk.** 1994. The mechanism of transposition of Tc*3* in *C. elegans*. Cell **79:**293–301.
64. **Weil, C. F., and R. Kunze.** 2000. Transposition of maize Ac/Ds transposable elements in the yeast *Saccharomyces cerevisiae*. Nat. Genet. **26:**187–190.
65. **Yant, S. R., A. Ehrhardt, J. G. Mikkelsen, L. Meuse, T. Pham, and M. A. Kay.** 2002. Transposition from a gutless adeno-transposon vector stabilizes transgene expression in vivo. Nat. Biotechnol. **20:**999–1005.
66. **Yant, S. R., L. Meuse, W. Chiu, Z. Ivics, Z. Izsvak, and M. A. Kay.** 2000. Somatic integration and long-term transgene expression in normal and haemophilic mice using a DNA transposon system. Nat. Genet. **25:**35–41.
67. **Yoder, K. E., and F. D. Bushman.** 2000. Repair of gaps in retroviral DNA integration intermediates. J. Virol. **74:**11191–11200.
68. **Zagoraiou, L., D. Drabek, S. Alexaki, J. A. Guy, A. G. Klinakis, A. Langeveld, G. Skavdis, C. Mamalaki, F. Grosveld, and C. Savakis.** 2001. In vivo transposition of Minos, a *Drosophila* mobile element, in mammalian tissues. Proc. Natl. Acad. Sci. USA **98:**11474–11478.
69. **Zhang, G., V. Budker, and J. A. Wolff.** 1999. High levels of foreign gene expression in hepatocytes after tail vein injections of naked plasmid DNA. Hum. Gene Ther. **10:**1735–1737.
70. **Zhong, Q., C. F. Chen, P. L. Chen, and W. H. Lee.** 2002. BRCA1 facilitates microhomology-mediated end joining of DNA double strand breaks. J. Biol. Chem. **277:**28641–28647.